POLINA LEMENKOVA
https://orcid.org/0000-0002-5759-1089
Schmidt Institute of Physics of the Earth, Russian Academy of Sciences
Laboratory of Regional Geophysics and Natural Disasters (No. 303)
10 Bolshaya Gruzinskaya St., Bld. 1, Moscow, 123995, Russia
pauline.lemenkova@gmail.com

Geomorphology of the Puerto Rico Trench and Cayman Trough in the Context of the Geological Evolution of the Caribbean Sea

Geomorfologia Rowu Puerto Rico i Rowu Kajmańskiego
w kontekście ewolucji geologicznej Morza Karaibskiego

Abstrakt: W artykule opisano badania wybranych elementów rzeźby dna Morza Karaibskiego na tle budowy geologicznej, tektoniki oraz wybranych właściwości pola geofizycznego wpływającego na powstawanie rowów głębinowych. Analizę batymetrii wzdłuż Rowu Puerto Rico i Rowu Kajmańskiego wykonano z wykorzystaniem mapowania tematycznego, modelowania geomorfologicznego i analizy statystycznej. Wykorzystano zestaw narzędzi do tworzenia skryptów kartograficznych w środowisku Generic Mapping Tools (GMT). Dane obejmują numeryczny model batymetryczny o strukturze GRID z bazy GEBCO, globalny model geopotencjału EGM2008, anomalie grawitacyjne z uwzględnieniem redukcji wolnopowietrznej (redukcja Faye'a) z połączonego zestawu danych altymetrycznych z misji GEOS3/SEASAT/GEOSAT, numeryczny model miąższości osadów o strukturze GRID i rozdzielczości 5 minut z programu GlobSed oraz warstwy wektorowe w formacie GMT (linie brzegowe, sieć rzeczna, granice). Przekrój został wykonany z wykorzystaniem modułu „grdtrack". Wyniki pokazały różnice między strukturą Rowu Puerto Rico i Rowu Kajmańskiego, na które wpływ miała ewolucja geologiczna. Średnie nachylenie zboczy rowu Puerto Rico (67,5°W i 19,90°N do 64,1°W i 19,82°N) wynosi 13°. W części północnej zbocza są bardziej strome (32,09°), ale wyższe na zboczu kontynentalnym. Profile Rowu Puerto Rico są asymetryczne dla obu boków z powodu uskoków i ruchów tektonicznych płyty karaibskiej i płyty północnoamerykańskiej. Dno morskie Rowu Kajmańskiego jest płaskie w tym segmencie (80,0°W i 17,70°N do 78,5°W i 19,50°N). Jego profil jest asymetryczny: północna część jest stroma (57°), a południowa jest bardziej łagodna (16°). Bardzo duże ujemne anomalie grawitacyjne Faye'a na wolnym powietrzu (do −380 mGal) widoczne są w Rowie Puerto Rico, na południe od Kuby oraz w północno-wschodniej części Rowu Kajmańskiego. Subdukcja płyt tektonicznych w Małych Antylach, Ameryce Środkowej i na dnie morskim, obejmująca nieckę kajmańską, koreluje ze zmianami falowania geoidy wywołanymi właściwościami skał powodujących anomalie

grawitacyjne. Analiza warunków topograficznych na przekroju podłużnym ujawnia różnice dla Rowu i niecki. W przeciwieństwie do Rowu Puerto Rico z wyraźnym pikiem gęstości (680 próbek dla głębokości od –5200 do –5400 m), Rów Kajmański ma bimodalny rozkład danych: dwa szczyty odpowiadają dwóm interwałom: 1) od –3250 m do –1000 m; 2) od –5250 m do –3500 m. Wnioski zawarte w artykule mogą przyczynić się do badań geologicznych Morza Karaibskiego z technicznym zastosowaniem GMT do modelowania geomorfologicznego.

Słowa kluczowe: globalny model geopotencjału; anomalie grawitacyjne; GMT; Rów Kajmański; Rów Puerto Rico; Morze Karaibskie

Abstract: This paper concerns the Caribbean Sea submarine geomorphology and bathymetry and especially the Puerto Rico Trench and the Cayman Trough, using thematic mapping, geomorphological modelling and statistical analysis. The technical tools include Generic Mapping Tools (GMT) cartographic scripting toolset. The data include GEBCO digital bathymetric model in grid format, geopotential model of the Earth's gravity field EGM2008, marine free-air Faye gravity anomalies from a combined GEOS3/SEASAT/GEOSAT altimeter data set, sediment thickness from the GlobSed 5-arc-minute grid model and vector layers of GMT (coastlines, river network, borders). The cross-sectioning was done by the "grdtrack" module. Differences between the form of the Puerto Rico Trench and Cayman Trough presumably result from different structure and geological evolution. The geomorphology of the segment of the Puerto Rico Trench (67.5°W and 19.90°N to 64.1°W and 19.82°N) has a gentle curvature of the slope in plane (about 13° slope steepness). The slopes are steeper in the northern part (about 32°) but higher on the continental slope. The profiles of the Puerto Rico Trench are asymmetric due to the tectonic factors. The seabed of the Cayman Trough is flat at the segment (80.0°W and 17.7°N to 78.5°W and 19.5°N). Its profile is asymmetric: northern part is steep (about 57°), southern part is about 16°. A very large negative Faye free-air gravity anomaly (up to –380 mGal) is seen in the Puerto Rico Trench, south of Cuba as well as in the north-eastern part of the Cayman Trough. The tectonic plate subduction in the Lesser Antilles, Central America and seafloor spreading is reflected in the morphostructure in the Cayman Trough and Puerto Rico Trench. Modeled cross-sectioning profiles show differences both for the Trench and Trough. In contrast with the Puerto Rico Trench with distinct density peak (680 samples for depths –5,200 to –5,400 m), the Cayman Trough has a bimodal data distribution: two peaks correspond to the two intervals: 1) –3,250 m to –1,000 m; and 2) –5,250 to –3,500. The paper contributes to Caribbean Sea geological studies by using GMT for geomorphological modelling.

Keywords: Earth gravitational model; gravity anomalies; GMT; Cayman Trough; Puerto Rico Trench; Caribbean Sea

INTRODUCTION

This paper is focused on the Caribbean Sea region and the analysis of its geologic and tectonic structure with regard to the seabed geomorphology. The Caribbean Sea is composed of several major topographic and geologic provinces (Holcombe *et al*. 1990), the spatial relationships of which are illustrated in Figure 1. Earlier works on the Caribbean Sea and marine mapping of other basins are presented in various papers which were mainly based on the available data and

various methods of cartographic mapping (e.g. Heezen, Tharp 1961; Case *et al*. 1984; EEZ-Scan 85 Scientific Staff 1987; Edgar *et al*. 1990; Gauger *et al*. 2007; Collina-Girard 2002; Klaucke *et al*. 2008; Clay *et al*. 1964; Lemenkova 2011; Belderson *et al*. 1972; Kuhn *et al*. 2006; Suetova *et al*. 2005; Wille 2005). The specific focus of this paper is to compare the submarine geomorphology of the Puerto Rico Trench and the Cayman Trough, two morphological features of the seafloor of the Caribbean Sea. Normally, trenches are located at the convergent tectonic plate boundaries. In general terms, oceanic trenches are defined as the deepest topographic depressions, narrow, long, with V-shape or U-shape form in a perpendicular cross-section (Shepard 1963). However, the variety of their forms is diverse reflecting the local specific of the geological conditions and evolution of the tectonic processes.

The Caribbean Sea is bounded from the north and east by the arc of the Greater Antilles (including Cuba, Hispaniola, Puerto Rico, Jamaica, and the Cayman Islands) and eastern group of the Lesser Antilles (including Windward Islands, Leeward Islands, and Leeward Antilles). The southern branch of the Lesser Antilles (Leeward Islands) is located on the submarine ridge stretching along the coast of Venezuela. The sub-latitudinal branches of the arc ridge (northern and southern) are composed of the Meso-Cenozoic structures divided by the oblique faults into a number of blocks. Its eastern arcuate branch is formed by a massive block with a convex surface (depths of –600 to –700 m), where numerous volcanic islands are located. A second chain of small limestone islands is located in the northern part of the Antilles island arc on a volcanic basement. The Puerto Rico Trench stretches from the outside of the Antilles ridge (Fig. 1 and 2). Its seafloor bottom is formed by a chain of narrow depressions with a flat topography, separated by several gentle steps. The slopes of the trench are steep, complicated by steps and short lateral ridges, which indicates to certain tectonic disturbances in this area. The trench is replaced by a massive submarine Barbados Ridge southward of Guadalupe Island. The Barbados Ridge is separated from the arc of the Lesser Antilles by a small Tobago Basin with depths up to –2,579 m.

The structure of the Caribbean Sea has a complex morphological character due to its origin: it is formed under condition of the movement of the Caribbean Plate subducting under the island arc separated from the continent by the basin of the Caribbean Sea (Ladd *et al.* 1990). The Caribbean Sea is a marginal sea which has an elongated shape along the Antilles island arc. Its depths are comparable with the depths similar to that of the oceanic depressions (from –3,000 to –5,000 m). The deepest point (7,686 m) occurs at the Cayman Trough, a narrow trough trending NE to SW with a total opening of about 1,100 km (Rosencrantz *et al*. 1988; Rosencrantz, Sclater 1986; Rosencrantz, Mann 1991).

Fig. 1. Topographic map of the Caribbean Sea basin (Source: Own study)
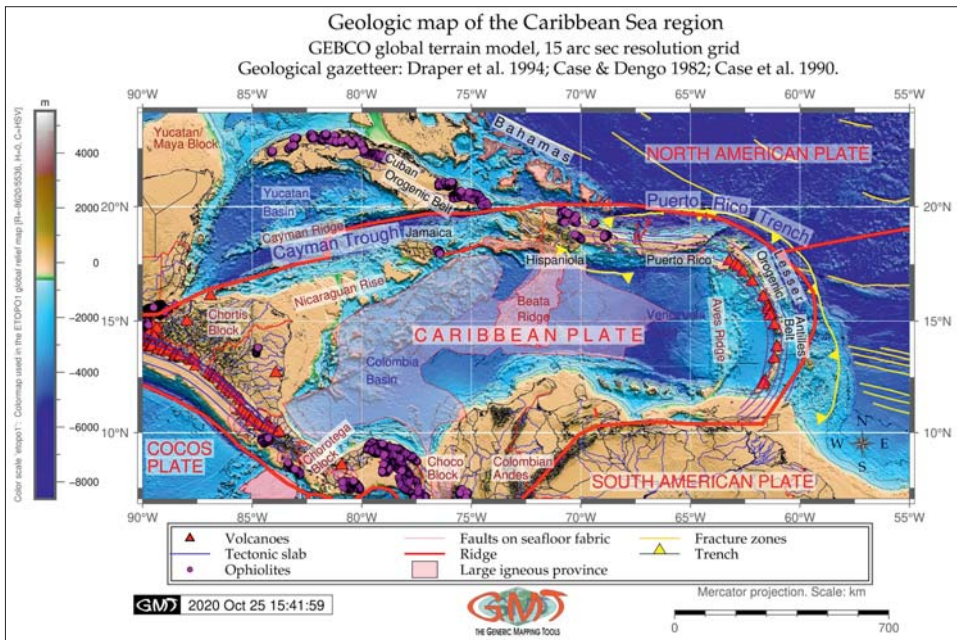

Fig. 2. Geologic map of the Caribbean Sea basin (Source: Own study)

The submarine geomorphology of the Caribbean Sea is notable for presence of submarine plateaus and ridges, dividing it into a series of smaller depressions. These uplifts and elevations result from various tectonic movements. The basin of the Caribbean Sea is a relics of the ocean seafloor, separated from the ocean by the Antilles island arc.

Rapid development of the Greater Antilles geosyncline in the Caribbean Sea region took place during Late Cretaceous and Early Paleogene (Pindell, Barrett 1990). The period of subduction was followed by the orogenesis, which was characterized by the deformations, granitoid intrusions and the uplift of the Antilles. Early basaltic volcanism was replaced by the andesite volcanism (Bandy 1970). The bottom of the basins created earlier continued to sink while North American Plate and South American Plate were moving apart. This was accompanied by the overthrusts directed towards the Florida/Bahamas platform in the north and South American Platform in the south. The Caribbean Plate moved eastward, about the opposite direction to the movement of the Atlantic oceanic lithosphere (Bracey, Vogt 1970).

The Puerto Rico Trench was formed as a result of these processes in the Wadati–Benioff zone along the eastern edge of the Antilles arc. The Grenada Basin was formed in the Eocene when the arc of the Lesser Antilles moved eastward. In general, the early Paleogene is characterized by a predominance of the horizontal movements in the Caribbean Plate region. Further discussions on the geologic setting in the Caribbean Sea regions are given in both previously published works and in recent studies (Jamieson *et al*. 2020; Schmidt, Siegel 2011; Shibata 1979; Beets *et al*. 1984; Meschede, Frisch 2002; Case *et al*. 1971; Case, MacDonald 1973; Perfit *et al*. 1980).

The tectonic history of the Caribbean Sea is strongly affected by the lithospheric plate movements (Burke *et al*. 1984). The continents of North and South America began to move apart in the Jurassic period along with the opening of the Atlantic Ocean (Sclater *et al.* 1977). At the same time, the Yucatán Block and Chortis Block off southern Mexico including Central American regions: Honduras, Nicaragua, El Salvador and Guatemala (Keppie, Morán-Zenteno 2012) that were previously sandwiched between them, began to rotate clockwise. During Cretaceous period, when the Greater Antilles geosyncline (island arc) enveloping the Caribbean Plate was formed, the Caribbean Plate began to move eastward towards the South American Plate (Aggarwal 1983). This resulted in the formation of the Wadati–Benioff zone, along which the Puerto Rico Trench and the Barbados Ridge were finally formed (Protti *et al*. 1994; Hayes *et al*. 1986). The Wadati–Benioff zone indicates the area where intermediate and deep-focus earthquakes (depths of 700 km) accompany downgoing slabs affected by high

pressure and temperature (Brodholt, Stein 1988). This eventually results in the high seismicity and volcanism of the Caribbean and south Mexican region (Carr, Stoiber 1990; Alaniz-Álvarez *et al*. 2002). The horizontal movements continued in the Paleogene, but vertical tectonic movements began to prevail during the Neogene. The seismicity and kinematics of the Caribbean presents a complex picture of tectonic movements including strike-slip motion and frontal subduction. More specifically, the region of the Caribbean–North America plate boundary is notable for a specific example of transition of the tectonic movements which gradually changes in the west direction: the along-strike transition from normal plate subduction in the Lesser Antilles is followed by an oblique subduction in Puerto Rico, then to strike-slip motion along the southern boundary of the Caribbean plate in South America and finally oblique collision in Hispaniola (Calais *et al*. 2016). Such variability in tectonic movements reflects the geological segmentation resulted from the evolution history of the plate boundary.

DATA AND METHODS

The present study is based on the Generic Mapping Tools (GMT) cartographic scripting toolset developed and maintained by Wessel and Smith (1991). Current study utilizes version 6.0.0 of GMT (Wessel *et al*. 2019). Topographic mapping (Fig. 1) was based on GEBCO digital bathymetric model with a grid spacing of at 15 arc-second intervals (GEBCO Compilation Group 2020) by methodology of GMT scripting through series of modules (Wessel *et al*. 2013; Lemenkova 2019a). For instance, the following methods were used to prepare a topographic map: the "grdcontour" module of GMT was used to add contour lines using the grid in NetCDF format (cs_relief.nc). The region was defined as the "-R270/305/7/24" flag where the west/east coordinates are given in 360° (that is, from 90 to 55 W), and south/north coordinates are from 7 to 24. The projection is defined in the "-JM6i" flag, the hillshade is added using topographic illumination "-I+a15+ne0.75" in a "grdimage" command. The "grdimage" processes the grid file (NetCDF) and produces a shaded relief map by plotting rectangles centered on each grid node in a NetCDF file. Then each pixel is assigned a color-shade value based on the *z*-value in a grid. The shaded relief was applied using the "-I" flag which processes a grid file with a constant intensity (in this case, +a15 means an azimuth of 15° for the shaded effect), affecting the ambient light. The GMT uses "greenspline" for slope calculation and direction approximation, for instance, by curvature splines for surface modelling from the input data in.txt format. The GMT "grdgradient" is designed to compute the directional derivative or to find the magnitude in a given slope direction of the

topographic data. The GEBCO digital bathymetry model (https://www.gebco.net/) itself is based on using the SRTM digital elevation model and bathymetry satellite altimetry data (Smith, Sandwell 1997). Other sources of geological and tectonic data available as base layers (maps) in GMT are as follows (last access date to all the web-links: 24.10.2020):

1. Tectonic datasets: http://www.soest.hawaii.edu/PT/GSFML/ML/index.html

2. Gravity data: https://www.earthbyte.org/category/resources/data-models/gravity/

3. Geological datasets: https://www.earthbyte.org/category/resources/

4. Geophysical data EGM2008: http://earth-info.nga.mil/GandG/wgs84/gravitymod/egm2008/index.html

5. Sediment thickness: https://ngdc.noaa.gov/mgg/sedthick/

Geological and tectonic mapping (Fig. 2) is based on embedded data in GMT. For instance, coastlines, political borders, rivers were added on the map using "pscoast" module. Vector layers containing geological data were visualized by the "psxy" GMT module using the described script (Lemenkova 2019c). Additional geological data were added from the extensive publications on the geology of the Caribbean Sea (Draper *et al*. 1994; Case, Dengo 1982; Case *et al*. 1990). Generalization of the geological data aimed to isolate the spatial characteristics from the thematic phenomenon of the geologic information (faults, blocks, fracture zones, volcanoes, ophiolites), by reducing the information for
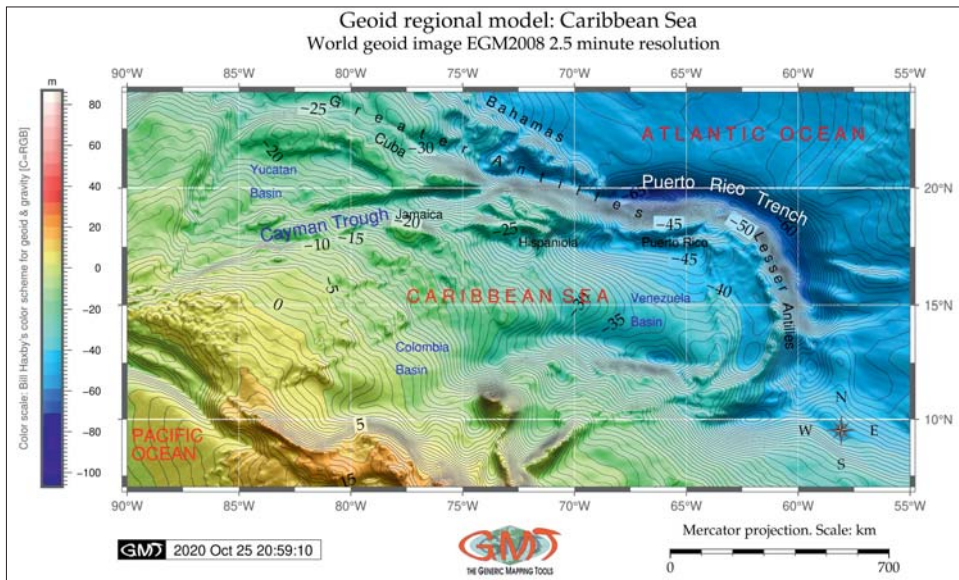

Fig. 3. Geoid model of the Caribbean Sea basin (Source: Own study)

the targeted map (Fig. 2). Hence, the principal goal of the thematic generaliza-tion was to reduce the number of minor geological objects, to visualize major geological objects and the most important geological features and settings in the Caribbean Sea region affecting the formation of the Puerto Rico Trench and the Cayman Trough.

A geopotential model of the Earth's gravity field EGM2008 used as a base raster dataset for modelling geoid (Fig. 3) of the Caribbean Sea (Pavlis *et al.* 2012), which is an improved and updated version of geoid with finer resolu-tion (2.5-minute resolution) of the EGM96 (15-minute resolution) (Lemoine *et al.* 1998). The scripting was mainly based on GMT module "grdimage" using described listing (Lemenkova 2019b). The assessment of the data range (ma-ximum/minimum) was performed by GDAL library (GDAL/OGR contributors 2020) through its utility "gdalinfo": gdalinfo EGM2008cs.grd -stats. Gravity anomalies and sea surface heights (Fig. 5) have been computed on a 0.125° grid in the ocean areas from a combined GEOS3/SEASAT/GEOSAT altimeter data set and data on marine gravity anomaly from Geosat and ERS 1 satellite altimetry (Sandwell, Smith 1997). This data base was received in March 1993 and processed by Scripps Institution of Oceanology (Sandwell *et al.* 2014). The area of data coverage is global (latitude 72N to 72S and longitude 0E to 360E) which was then subset for the current region of the Caribbean Sea (90°W–55°W, 7°N–25°N) using GMT scripting approach. Cartographic layout and plotting was made using applied methods (Lemenkova 2019g; Wessel, Smith 2018).

The sediment thickness of the Caribbean Sea seafloor (Fig. 4) was visualized using "GlobSed", a new global 5-arc-minute total sediment thickness model in a NetCDF format (GlobSed-v2.nc) which covers the world's oceans and marginal seas (Straume *et al.* 2019). Technically, modelling the seafloor segments through transecting the Trench and the Trough by bathymetric profiles was done using a sequence of the GMT modules, and Unix progs (echo, rm, cat). The cross-track profiles were generated as 300 km long, spaced 20 km, sampled every 2 km lines and stacked using the median by GMT module "grdtrack". The cross-sections were prepared in a direction perpendicularly to the morphological axis of the analyzed Trench and Trough. Although the trend of the axis in both cases is not truly linear, it displays a general curvature of the profiles. The plotting was done automatically using the following command: -C300k/2k/20k+v. Here the program specifies the distance between the samples, the interval between the lines of the profiles and the extent of the line, drawn and digitized automatically in a GMT.

Since the topographic data reflect the distance from the middle of each cross-section line, the coordinates were selected in the trench and trough axis, respectively: 85°W and 17.7°N to 78.5°W and 19.5N for the Cayman Trough,
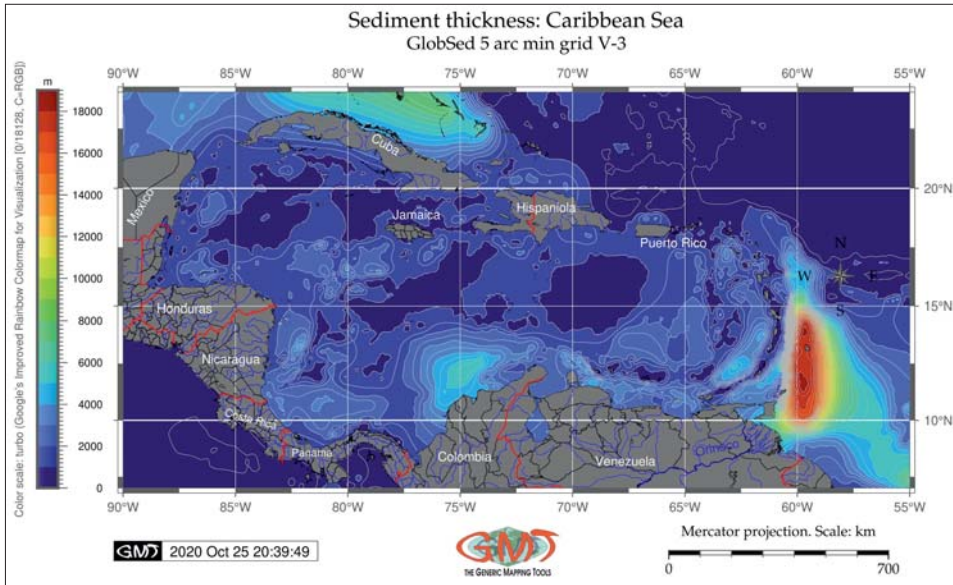
Fig. 4. Sediment thickness of the Caribbean Sea basin (Source: Own study)

and 67.5°W and 19.9°N to 64.1°W and 19.82°N for the Puerto Rico Trench. This information was then used in the visualization of their statistics. This table was then used for the statistical analysis and plotting the histograms. Thus, the tables with depth values for the Puerto Rico Trench and the Cayman Trough were written as stacked profile and processed by the "pshistogram" module of GMT. As a result, the cross-sections for the Puerto Rico Trench and the Cayman Trough are plotted as independent graphic representations of the intersection of the submarine geomorphology of the seafloor with a vertical plane of an axe orientation along the Trench and the Trough. The cross-sections of the terrain show different types of geomorphic structure in the Puerto Rico Trench and the Cayman Trough, as well as the topographic constitution of the relief.

The internal structure of both objects differ significantly, due to the geometric variability between the represented relief. It is an approximate model of the real distribution of the geomorphology of both submarine structures, based on the modeled data of GEBCO grid. It can also represent the extension of the materials of the structures that have been eroded above the topographic surface. The construction of the cross-sections required the application of a series of GMT modules as steps and the use of specific modules, such as "psxy" for plotting the line and two points, starting and end point: (gmt psxy -Rcmt_relief. nc -J -W2p,red trenchCMT.txt -O -K >> $ps') and (gmt psxy -R -J -Sc0.15i
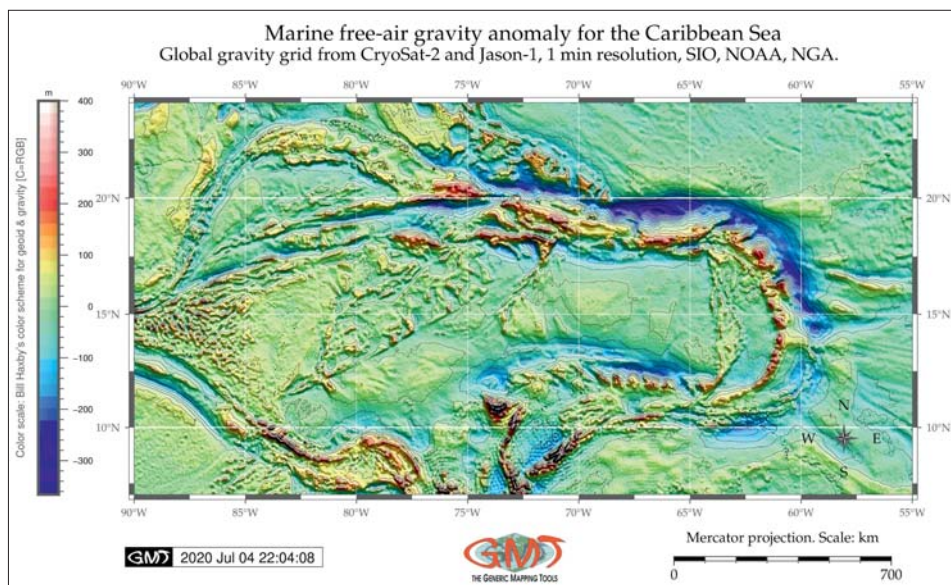
Fig. 5. Marine free-air gravity map of the Caribbean Sea basin (Source: own study)

-Gred trenchCMT.txt -O -K >> $ps). In order to reduce the degrees of variation in the profiles arrangement and to ensure the reliability of the cross-sections, the GMT techniques was applied for automatic cross-sectioning. In contrast with the other approaches, this part of the research was done automatically by the following line: "gmt grdtrack trenchCMT.txt -Gcmt_relief.nc -C300k/2k/20k+v -Sm+sstackCMT.txt > tableCMT.txt". Due to the importance of this code snippet, it is presented here in full. Afterwards, the digitized set of profiles of the Puerto Rico Trench (Fig. 6B) and the Cayman Trough (Fig. 7B) forms an array which was then saved for each corresponding structure as a csv table.

RESULTS

The presented paper resulted in a series of the thematic maps, two geomorphological models as graphical plots and a descriptive statistical analysis of the depths. Fig. 1 shows the topographic and bathymetric maps of the selected geomorphic features from the global seafloor features covering the Caribbean Sea region. Among others, it shows the distribution of the Cayman Trough and the Puerto Rico Trench, the sub-division of the Caribbean Sea into three basins (Venezuela, Colombia and Yucatán), continental shelf as well as the location of Greater and Lesser Antilles correlating with the tectonic plate borders (Fig. 2).

The geologic map presented in Fig. 2 shows the location, distribution and direction of main geological structures and features, such as faults, ridges, fracture zones, location of the ophiolites.

The tectonic processes and slab subduction combined with strong volcanic activities and earthquakes often lead to gravitation failure of the continental slope at the Trench inner slope. As can be seen (Fig. 2), the Lesser Antilles Orogenic Belt is bordered by a chain of volcanoes on the inner side of the trench. Comparison of the bathymetric and tectonic features in the study area can be performed. Fig. 2 illustrates the complexity of the Caribbean Sea which is a geologically diverse region including a variety of plate boundary interactions. The border of
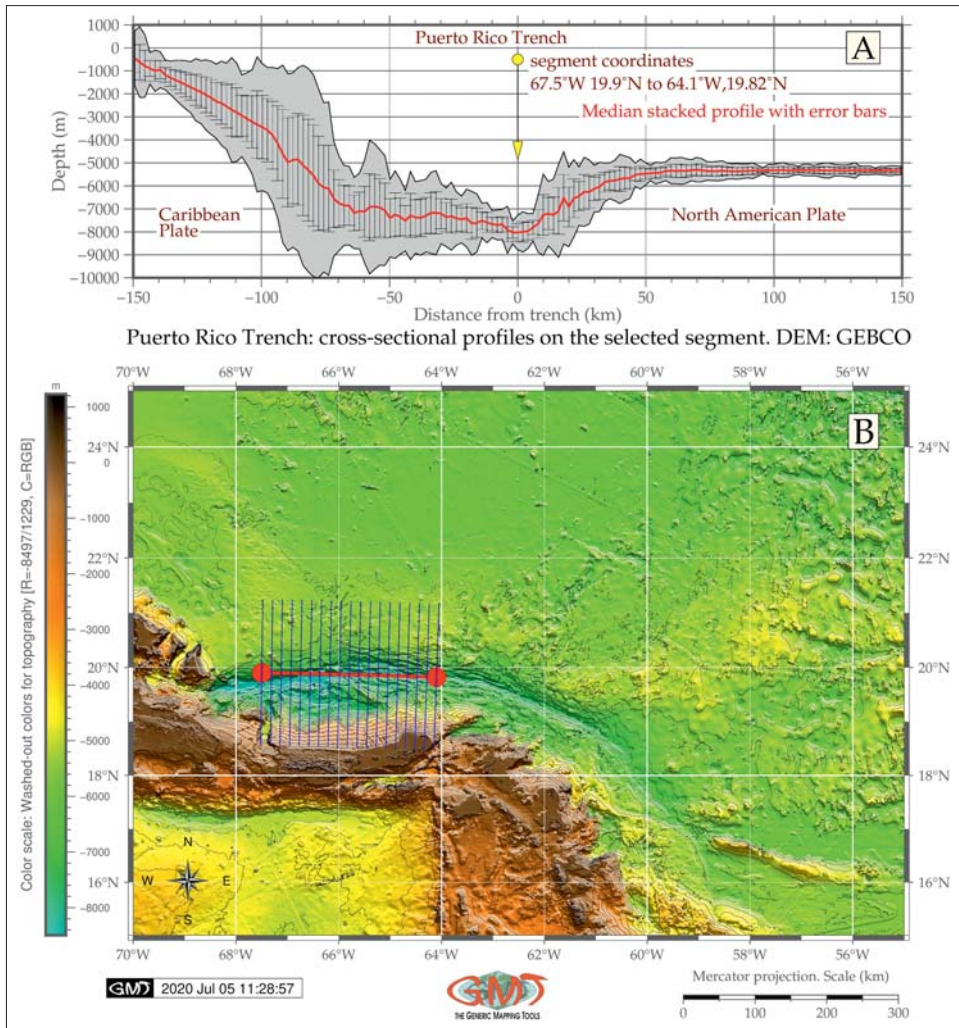

Fig. 6. Segments of the cross-section profiles of the Puerto Rico Trench (Source: Own study)

the tectonic plates (red thick line in Fig. 2) shows the tectonic plate subduction in the Lesser Antilles and Central America and seafloor spreading in the Cayman Trough.

The Caribbean Sea includes several deeper water sub-basins: the Yucatán Basin, the Cayman Trough, the Colombian Basin, the Venezuelan Basin and the Puerto Rico Trench (Fig. 1 and 2). The basins are separated by ridges and rises: the Cayman Ridge, the Nicaraguan Rise, the Beata Ridge and the Aves Ridge (Fig. 1 and 2). The Beata Ridge trends south-west from Cape Beata, Hispaniola, for about 400 km. The ridge has a relief of about 2,000 m (light aquamarine color in Fig. 2).
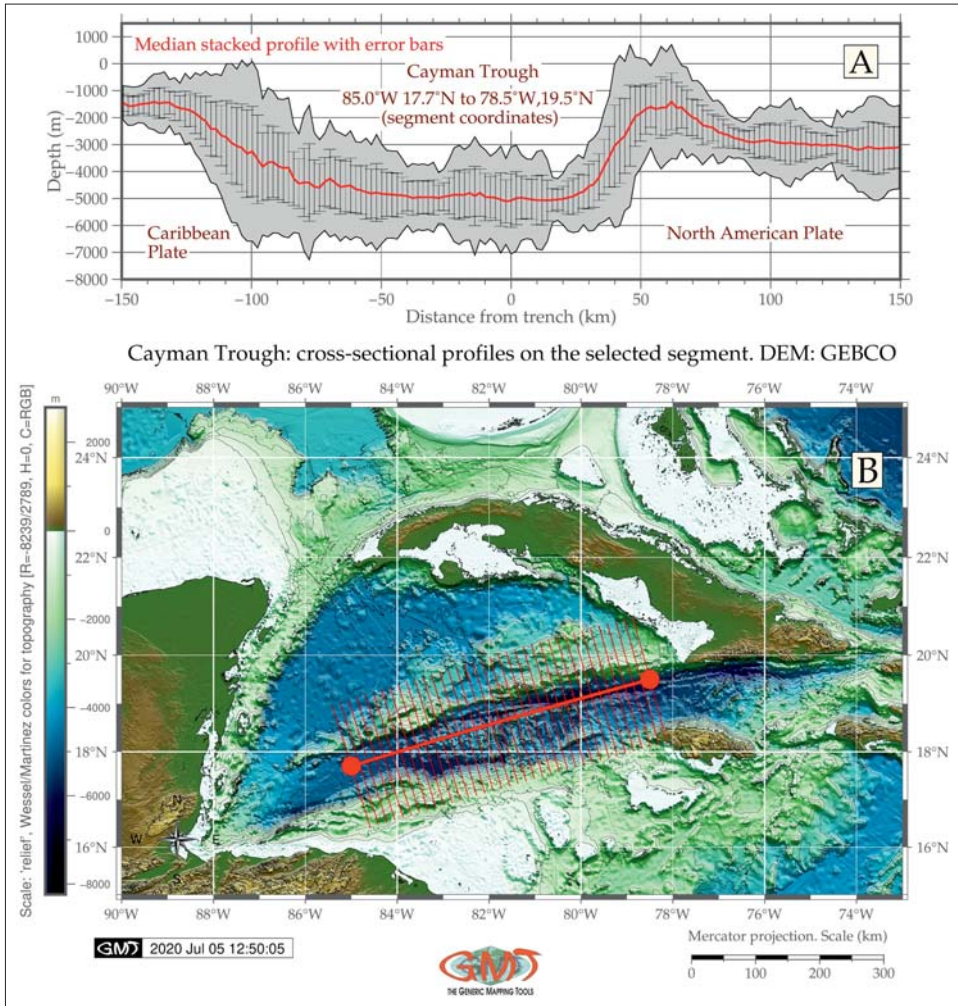

Fig. 7. Segments of the cross-section profiles of the Cayman Trough (Source: Own study)

The Colombian basin extends to depths of 4,000 to 4,400 m (blue colors, Fig. 1) and occupies the largest abyssal plain in the Caribbean Sea region. However, the deepest bathymetric unit in the study area is the Venezuelan Basin, separated from the Colombian basin by the Beata Ridge. As can be seen on the GEBCO based bathymetric map (dark blue colors, Fig. 1), the basin relief is leveled, with a "smoothing" effect, which results from the accumulated sediments (Fig. 1). The Lesser Antilles is composed of a series of volcanic islands in the form of arc extending northward at 850 km (Fig. 2). Fig. 3 illustrates the geoid model of the Caribbean Sea basin. The sediment thickness in the Caribbean Sea is up to 4–5 km (blue areas, Fig. 4). About half of the upper layer is presented by loose sediments, according to Lisicyn (1974). The largest sediment sources in the Caribbean Sea include the Magdalena River, the largest river discharging sediments in the basin with the rate of sedimentation 560 t km^2 $year^{-1}$) (Caribbean Sea Ecosystem Assessment Team 2007), and rivers of the Orinoco Basin (Gomez 1996). As can be seen in Fig. 4, the thickness of sediment layer increases in the area of the Lesser Antilles (orange to red areas, Fig. 4). The specific data distribution shows that the sedimentation is higher on the Atlantic Ocean side up to 5–8 km thickness (light green "plume" from the Lesser Antilles) decreasing from their Caribbean Sea side to 3–4 km of layer thickness. In the Puerto Rico Trench, the thickness of sediment layer increases to 4 km (blue colors, Fig. 4), rapidly decreasing up to 500–1,000 m in the open areas of the Caribbean Sea (dark blue color, Fig. 4). The Cayman Trough demonstrates middle values of the sediment thickness reaching up to 3 km of thickness layer.

The free-air Faye gravity anomalies spatially vary in the Caribbean Sea: in the Venezuelan Basin, the values are about –20 mGal, in the Colombian Basin, they differ from –4 to +26, in the Yucatán Basin – about –6 mGal (light green areas, Fig. 5). A very large negative Faye free-air gravity anomalies (up to –380 mGal) are confined to the Puerto Rico Trench (dark blue areas, Fig. 5) and south of Cuba at the north-eastern part of the Cayman Trough (blue areas, Fig. 5). Extremely low gravity anomaly in the Puerto Rico Trench has also been proved in previous studies (ten Brink 2005). The axis of the Faye gravity anomaly in general coincides with the axis of the Puerto Rico Trench and the "borders" of the Cayman Trough, but is slightly moved to the slope of the island arc of the Lesser Antilles (orange to red colors corresponding to the values of above 100 mGal, Fig. 5). This can be explained by the inclined position of the deep fault along which the Puerto Rico Trench is formed. Repeating the geometric shape form of the arc of the Lesser Antilles, the zone of Faye gravity negative anomalies moves then southward to the Barbados Ridge, rising from the southern end of the Puerto Rico Trench axis, which emphasizes the structural geologic

relationship between them. Further studies detailing geophysical setting in the Caribbean region can be found in the literature (Couch, Woodcock 1981; Roobol *et al*. 1983; Calais, Mercier de Lepinay 1991; Pinet 1976). Regional studies, for instance, report positive Bouguer anomalies, suggesting a relatively thin continental crust and a lack of isostatic balance in the basin of the north Columbia (Case, MacDonald 1973).

Fig. 6 and 7 show the resulting transects of the seafloor geomorphology of the Puerto Rico Trench and Cayman Trough, the Caribbean Sea. Both Puerto Rico Trench and Cayman Trough are notable comparing to other trenches, due to its specific trough-shaped irregular form. For instance, other trenches, e.g. Mariana, Kuril-Kamchatka Vityaz, Vanuatu, Izu-Bonin (Lemenkova 2020a, 2020b), have V- or U-shaped cross sections. The cross-section of the Cayman Trough (Fig. 7) is not typical for trenches. This may be a consequence of sediment cover masking the original bathymetry developed as a typical trench during earlier stages by subduction processes. As pointed by Harris and Macmillan-Lawler (2017), the age of the lithosphere plays a key role in the seafloor morphology. The ocean trench is a notable geomorphic feature of the "mature" category of the ocean seafloor (with the age of over 8 MA). The "mature" ocean basins are characterized by a thick sediment layer (ca. 940 m), high concentration of seamounts, presence of the deep-sea trench and large areas occupied by a continental rise (around 20%). Other factors reflected in structural variations along the Trough, suggested by Granja Bruña *et al.* (2009), include overburden of the asymmetrical thrust belt and variability of the crust.

The GlobSed-based isopach map displays relative greater sediment thickness of up to 3–4 km in the Cayman Trough and Puerto Rico Trench (Fig. 4). Nevertheless, even if the V-form typical for the oceanic trench is absent in both cases, the Puerto Rico Trench is classified as a trench in submarine geomorphology and the Cayman Trough is sometimes referred to as "trench" yet more often as "trough" (Perfit, Heezen 1978; Rosencrantz *et al*. 1988; Rosencrantz, Mann 1991). Both terms were also used indistinctly for the Muertos depression located to the south of the Hispaniola and Puerto Rico islands (Granja Bruña *et al*. 2009).

The Puerto Rico Trench and Cayman Trough present a geomorphology formed in the process of the oceanic plates subduction. The maximum depth of the Puerto Rico Trench is –8,497 m according to the GEBCO digital bathymetric model with a grid spacing of 15 arc-seconds. This is an asymmetric structure, where slopes show tendency to be steeper and lower in its northern part and gentle but higher in the southern part (Fig. 6A and B). The inner trench wall is composed of a variety of rocks, such as marble, calc-schist, mica-schist, greenschist, amphibolite, magnesian schist and serpentinite, while the dredge from
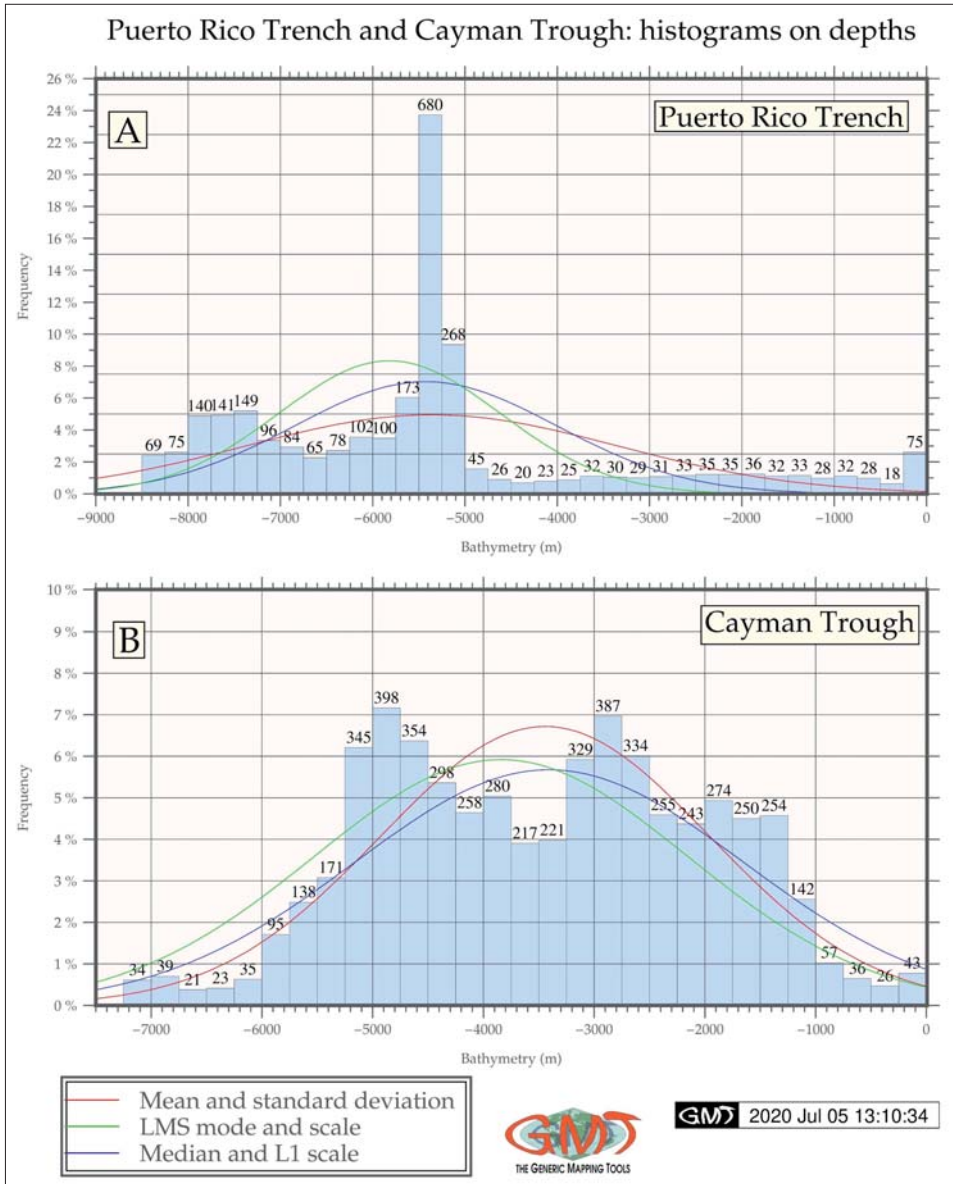
Fig. 8. Statistical histograms of the cross-section profiles: Cayman Trough and Puerto Rico Trench (Source: Own study)

the outer wall (oceanic side) shows tholeiitic basalts, serpentinite and deep-sea sediments (Perfit *et al*. 1980). The geomorphology of the segment extending along the southern side of the Puerto Rico Trench (67.5°W and 19.90°N to 64.1°W and 19.82°N) is characterized by a gentle profile curvature (around 14°

slope steepness, Fig. 6). It has a clearly asymmetric form of both flanks due to faults and tectonic movements: the Caribbean Plate is moving eastward, while the North American Plate is moving westward.

The specifics of the asymmetry of the trench slopes is connected with the plate tectonics in this region, which can be illustrated by the variations in the velocity of plate movements: while the North American and South American plates have a low motion rate (Patriat *et al.* 2011), the Caribbean plate moves faster, at 18–20 mm/yr in the eastward direction (DeMets *et al.* 2000). This motion is slightly oblique to the plate boundary in Hispaniola, almost parallel to the Puerto Rico Trench, then its direction gradually becomes perpendicular to the trench in east and south direction in the Lesser Antilles. Thus, the Puerto Rico Trench is constrained by the highly obliquely convergent plate subduction in the north and by the left-lateral strike-slip fault in the south. This can cause the subsidence of its outer and inner walls and illustrate variations in bathymetry of the trench in its various segments.

The Cayman Trough extends a distance of ca. 1,600 km, has 120 km in width and 5 km in depth (Fig. 7). Topographically, the Trough extends south-westwards from the Windward Passage (74°W), separating Cuba and Hispaniola from the Gulf of Honduras (87°W). Geologically, the Cayman Trough separates the Cayman Ridge from the Nicaraguan Rise (Fig. 2). Its floor is composed of mafic and ultramafic rocks (Perfit, Heezen 1978). The bottom morphology is leveled here and the cross-sections are typical for the trough. The depths in the Cayman Trough are greater than in the Yucatán basin with the maximal depth at 8,239 m according to the GEBCO data modelling. Comparing to the Puerto Rico Trench, it is wider in a cross-section profile and has a leveled morphology due to the high sedimentation in the selected segment (80.0°W and 17.70°N to 78.5°W and 19.50°N, Fig. 7). The Trough has an asymmetric profile in a cross-section with a steeper slope in its northern flank (about 57°) and gentler (16°) in the southern one (Fig. 7A and B).

The histograms in Fig. 8 demonstrate the depth distribution frequency for the segments of the Puerto Rico Trench (Fig. 8A) and the Cayman Trough (Fig. 8B). The analysis for each cross-section profile indicates, based on the summarized data, the following results. For the Puerto Rico Trench, the most repetitive depth values are clearly located in a bin with a range of –5,200 to –5,400 m (680 samples) followed with a large gap by the intervals within depths from –5,000 to –6,000 m: intervals of –5,000 to –5,200 m (268 samples), –5,500 to –5,750 m (173 samples) and –5,750 to 6,000 m (100 samples). All other depths values are very insignificant comparing to the depth of 5,000 to –6,000 m (more exactly, all values from –5,000 m to 0 do not exceed 100 samples in each bin).

Thus, the most representative bathymetric data range for the Puerto Rico Trench is between –5,000 and –6,000 m.

As for the Cayman Trough, the data variations have completely different character. In contrast with the Puerto Rico Trench having a clear peak, the Cayman Trough has a bimodal depth distribution frequency. At first sight, it is clear the two peaks correspond to the two intervals: 1) –3,250 to –1,000 m; and 2) –5,250 to –3,500 m. The remaining data can be considered as insignificant as located on the slopes and crossing the submarine ridges. The most frequent bathymetric data for the Cayman Trough correspond to the bins of –4,750 to –5,000 m (398 samples) and –2,750 to –3,000 m (387 samples). In general, the data for the depths in a larger interval of below –1,000 m (142 samples) and ending with –6,000 m (95 samples) reflect the best performance in a topographic profile of the Cayman Trough.

In the context of regional analysis of topographic variations, the comparison of the statistical analysis demonstrates relatively wide character of data distribution for the Cayman Trough: a lot of data are "located" in this interval (–1,000 to –6,000), while the Puerto Rico Trench demonstrates a steeper decrease in depths reaching its peak between –5,000 to –6,000 m, as mentioned before. A comparison of descriptive statistics about depth frequency distribution between the structures of the Cayman Trough and Puerto Rico Trench shows that mean values (red line in both subplots, Fig. 8) reach their highest values in the quadrant between –3,000 to –4,000 m, and –5,000 to –6,000 m for the Puerto Rico Trench. The extended report includes the least median of squares (LMS) regression line, the L1 scale of the mode, i.e. central tendency and dispersion of the bathymetric data. The data comparison includes the LMS regression line estimator (a green line in the subplots in Fig. 8).

When comparing the least squares regression methods, the LMS is a more robust approach which uses the median of the squared residuals of the bathymetric data for estimation and corresponds to the narrowest strip covering about half of the observations (Rousseeuw 1984). Specifically, the highest values of the LMS for the Puerto Rico Trench (8.5%) is noted for the interval of –5,500 to –6,100 m, while the Cayman Trough has a peak at 5.9% at the depth values from –3,800 to –3,900 m. The median of the dataset (blue line in the subplots) shows the highest value (5.8% of all observations in a dataset) for the depths –3,300 to –3,500 m for the Cayman Trough and 7.5% of the data pool for the depths in the interval –5,400 to –5,600 m. The data distribution is illustrated by the bars showing the actual variability and frequency in a dataset.

The probability of the distribution of a bathymetric observation as a random variable against its mean shows the geomorphological asymmetry. Here the

Puerto Rico Trench demonstrates a unimodal distribution with positive skewness with the "tail" of the data pool on the right side of the distribution (the data above the –5,000 m on the subplot A). The Cayman Trough shows two peaks (–4,250 to –5,250 m and –2,500 to –3,250 m). The skewness of the data shows undefined deviations from the mean, since the small "tails" of the data pool are visible in both extreme negative data (below –6,000 m) and in the shallower areas (less than –1,000 m).

DISCUSSION

The presented research has demonstrated that complex processes are involved in geomorphological evolution of the oceanic seafloor and generating oceanic trenches and troughs. These include both geophysical processes that generate rock uplift and complex tectonic and geological processes that move and replace the rock. The processes interact in a complex way to generate composite bathymetry of the ocean seafloor. Based on the results, the major drivers of basin geomorphic evolution are tectonics (tectonic plates subduction, rates and direction), volcanism (intensity and repetitiveness) and sedimentation (which is expressed in sediment thickness of the seafloor). Tectonics actually gives rise to the Caribbean Sea basin in the first instance and continue governing its progress through the geologic evolution, which resulted in the formation of the Puerto Rico Trench and Cayman Trough through a complex process of plate subduction.

As pointed by Micallef *et al.* (2018), the main geomorphic expression of tectonism characterizing ocean basins is the percentage area of deep ocean trench, reflecting the subduction of oceanic crust along active margins. Trench area is correlated with the area of troughs in the ocean basins (Harris, Macmillan-Lawler 2017) which is explained by the fact that trenches partially infilled with sediment are in some cases transformed into troughs. This points out at the important correlation between the troughs and trenches in geomorphological classification of the submarine landforms. Indeed, comparing the presented geomorphology of the Puerto Rico Trench (Fig. 6) and the Cayman Trough (Fig. 7), the difference between their structure and forms are evident. The detected positive seismic anomalies under the Lesser Antilles and Puerto Rico are interpreted as remnants of Atlantic lithosphere subduction which confirms 1,100 km of tectonic convergence at the Lesser Antilles island arc during the past ~45 Myr (van Benthem *et al*. 2013). The North America lithosphere is subducting westward along the northeastern boundary of the Caribbean plate (Calais *et al*. 1992). This results in a formation of the northern Lesser Antilles slab which has a curved (amphitheater-like) geometry, which is continuous with the Puerto Rico slab along the

NE plate boundary. The Puerto Rico slab, in turn, is brought in by Eocene to present westward subduction at the Lesser Antilles island arc (Schell, Tarr 1978).

Calais *et al*. (2016) have recently shown a remarkable plate boundary segmentation in the northeastern Caribbean with variations in different parts of the region: Caribbean–North America plate boundary shows an along-strike transition from plate boundary to normal subduction in the Lesser Antilles, Puerto Rico shows oblique subduction with no strain partitioning, and area further west in Hispaniola shows oblique subduction and collision with strain partitioning. As a result, the differences in tectonic processes are mirrored in the submarine geomorphology of the oceanic seafloor. Variations of sediment flux and silicic lavas can also illustrate the tectonic models of the Caribbean evolution: in the western part of the central Puerto Rico, located further from the perpendicular subduction of the Caribbean spur of the mid-Atlantic Ridge, the heat flow is lower and produced limited crustal melting, while the sediment flux was comparatively elevated (Jolly *et al.* 2008). The impact of the volcanism and tectonics on geomorphology is reflected in the occurrence of various submarine landforms, such as oceanic trenches, mid-ocean spreading ridges, rift valleys and seamounts (Lemenkova 2018). Thus, seamounts are formed mainly along spreading ridges, situated nearer to the centre of the rift valley, located over the thinnest ocean crust (Wright, Rothery 1998).

CONCLUSIONS

Since the late 20th century, along with the rapid development of automatization, methods of numerical data modelling, data processing and progress in computer science, geologists have turned to the use of numerical models as a means of exploring the richness of the linkages between the geological processes and geomorphological landforms. The automatization necessarily mirrored in the development of the cartographic methods supported by the machine learning and statistics (Langlois, Phipps 1997; Schenke, Lemenkova 2008; Tsoulos, Stefanakis 2005; Klaučo *et al*. 2013a, 2013b; Tobler 1975, 1980; Lemenkova *et al*. 2012; Lemenkova 2019d). Along with the increased speed and memory size of computers, cartographic modelling have become more capable of treating the real-world complexity of the geological and geographic phenomena by discretizing space and time into smaller bites, operating with various data sources and formats, overlaying layers and performing complex statistical analysis of geospatial data (Thomas 2001; Lindh 2004; Lemenkova 2019e, 2019f; Sanders 1989; Klaučo *et al*. 2014, 2017).

Computer-based modelling in cartography allows understanding in a quantitative sense the linkages among the geological and geophysical processes that

result in modern topography of the seafloor. As demonstrated, the GMT provided a set of thematic geological and geophysical maps of how geological setting of the Caribbean Sea basin affected the formation of the submarine geomorphic landforms such as the Cayman Trough and the Puerto Rico Trench. Comparison of these maps with digital bathymetric models allows to perform a multivariable study on geological processes and geophysical conditions of the basin that are reflected in the submarine landforms, and contributes to the questions of how a particular submarine landform was formed and, in turn, how it is reflected in the modern geophysical fields. Embedding knowledge of ongoing geological and tectonic processes in a GMT scripting framework enables to increase our flawed understanding of these complex geological processes.

This paper analyzed the spatial pattern of bathymetric, geological and geophysical features of the Caribbean Sea and especially two regional structures – the Cayman Trough and the Puerto Rico Trench, and provided examples of depth frequency distribution based on arrays of geomorphological cross-sections. Geological and topographic maps were designed to illustrate the evolution of the individual landforms of the Caribbean Sea (faults, fracture zones, distribution and directions of depressions, elevations, seamounts, orogenic belts, ridges), cross-section models are aimed at demonstrating variations in the seabed morphology of the submarine landforms. Each of the maps was generated using a corresponding GMT script requiring a set of GMT modules. The goal of the presented research, including cartographic mapping, geomorphological modeling and statistical plotting, was to derive insights into the functioning of the many processes that contribute to generate submarine geomorphology of the Caribbean Sea of the Atlantic Ocean.

ACKNOWLEDGEMENTS

BIBLIOGRAPHY

Aggarwal Y. 1983. Present-day boundary and the motion of the Caribbean Plate relative to South America. *10th Caribbean Geological Conference*. Cartagena, Colombia, p. 16.

Alaniz-Álvarez S.A., Nieto-Samaniego A.F., Morán-Zenteno D.J., Alba-Aldave L. 2002. Rhyo-litic volcanism in extension zone associated with strike-slip tectonics in the Taxco region, southern Mexico. *Journal of Volcanology and Geothermal Research* 2483, 1–14. https://doi.org/10.1016/S0377-0273(02)00247-0

Bandy, O.L. 1970. Upper Cretaceous-Cenozoic paleobathymetric cycles, eastern Panamá and north-ern Colombia. *Gulf Coast Association of Geological Societies Transactions* 20, 181–193.

Beets D.J., Maresch W.V., Klaver G.Th., Mottana A., Bocchio R., Beunk F.F., Monen H.P. 1984. Magnetic rock series and high-pressure metamorphism as constraints on the tectonic history of the southern Caribbean. In: W.E. Bonini, R.B. Hargraves, R. Shagam (eds.), *The Caribbe-an-South American Plate Boundary and Regional Tectonics* (pp. 95–130). Geological Society of America Memoir 162.

Belderson R.H., Kenyon N.H., Stride A.H., Stubbs A.R. 1972. *Sonographs of the sea floor. A picture atlas*. Amsterdam: Elsevier. https://doi.org/10.1017/S0016756800038607

van Benthem S., Govers R., Spakman W., Wortel R. 2013. Tectonic evolution and mantle structure of the Caribbean. *Journal of Geophysical Research: Solid Earth* 118, 3019–3036. https://doi.org/10.1002/jgrb.50235

Bracey D.R., Vogt P.R. 1970. Plate tectonics in the Hispaniola area. *Geological Society of America Bulletin* 81, 2855–2860.

Brodholt J., Stein S. 1988. Rheological controls of Wadati–Benioff zone seismicity. *Geophysical Research Letters* 15(10), 1081–1084. https://doi.org/10.1029/gl015i010p01081

Burke K., Cooper C., Dewey J.F., Mann P., Pindell J.L. 1984. Caribbean tectonics and relative plate motions. *Geological Society of America Memoir* 162, 31–63.

Calais E., Mercier de Lepinay B. 1991. From transtension to transpression along the northern Ca-ribbean plate boundary off Cuba: Implications for the recent motion of the Caribbean plate. *Tectonophysics* 186(3–4), 329–350. https://doi.org/10.1016/0040-1951(91)90367-2

Calais E., Béthoux N., Mercier de Lépinay B. 1992. From transcurrent faulting to frontal subduc-tion: A seismotectonic study of the northern Caribbean plate boundary from Cuba to Puerto Rico. *Tectonics* 11, 114–123. https://doi.org/10.1029/91TC02364

Calais E., Symithe S., Mercier de Lépinay B., Prépetit C. 2016. Plate boundary segmentation in the northeastern Caribbean from geodetic measurements and Neogene geological observations. *Comptes Rendus Geoscience* 348, 42–51. https://doi.org/10.1016/j.crte.2015.10.007

Caribbean Sea Ecosystem Assessment Team. 2007. Caribbean Sea Ecosystem Assessment (CARSEA).

Carr M.J., Stoiber R.E. 1990. *Volcanism*. In: G. Dengo, J.E. Case (eds.), *The Geology of North America.* Vol. H: *The Caribbean Region* (pp. 365–392). Boulder: Geological Society of America. https://doi.org/10.1130/DNAG-GNA-H

Case J.E., Durán L.G., Alfonso López R.A., Moore W.R. 1971. Tectonic investigations in western Colombia and eastern Panama. *Geological Society of America Bulletin* 82, 2685–2712.

Case J.E., MacDonald W.J. 1973. Regional gravity anomalies and crustal structure in northern Co-lombia. *Geological Society of America Bulletin* 84, 2905–2916. https://doi.org/10.1130/0016-7606(1973)84<2905:RGAACS>2.0.CO;2

Case J.E., Dengo G. 1982. The Caribbean region. In: A.R. Palmer (ed.), *Perspectives in Regional Geological Synthesis: Planning for the Geology of North America* (pp. 163–170). Geological

Society of America. DNAG Special Publication, Vol. 1. https://doi.org/10.1130/DNAG-GNA-H

Case J.E., Holcombe T.L., Martin R.G. 1984. Map of geologic provinces in the Caribbean region. *Geological Society of America Memoir* 162, 1–30.

Case J.E., MacDonald W.D., Fox P.J. 1990. Caribbean crustal provinces: Seismic and gravity evidence. In: G. Dengo, J.E. Case (eds.), *The Geology of North America*. Vol. H: *The Caribbean Region* (pp. 15–36). Boulder: Geological Society of America. https://doi.org/10.1130/DNAG-GNA-H

Clay C.S., Ess J., Weisman I. 1964. Lateral echo sounding of the ocean bottom on the continental rise. *Journal of Geophysical Research* 69, 3823–3835. https://doi.org/10.1029/JZ069i018p03823

Collina-Girard J. 2002. Underwater mapping of late quaternary submerged shorelines in the Western Mediterranean Sea and the Caribbean Sea. *Quaternary International* 92, 63–72. https://doi.org/10.1016/S1040-6182(01)00115-X

Couch R., Woodcock S. 1981. Gravity and structure of the continental margins of southwestern Mexico and northwestern Guatemala. *Journal of Geophysical Research* 86, 1829–1840. https://doi.org/10.1029/JB086iB03p01829

DeMets C., Jansma P.E., Mattioli G.S., Dixon T.H., Farina F., Bilham R., Calais E., Mann P. 2000. GPS geodetic constraints on Caribbean-North America plate motion. *Geophysical Research Letters* 27(3), 437–440. https://doi.org/10.1029/1999GL005436

Draper G., Jackson T.A., Donovan S.K. 1994. *Geologic Provinces of the Caribbean Region*. Chapter 1: *Caribbean Geology: An Introduction* (p. 3). Kingston: U.W.I. Publishers' Association.

Edgar N.T., Dillon W.P., Jacobs C., Parsons L.M., Scanlon K.M., Holcombe T.L. 1990. Structure and spreading history of the central Cayman Trough. In: D.K. Larue, G. Draper (eds.), *Transactions of the 12th Caribbean Geological Conference* (pp. 33–42). St. Croix, U.S.V.L., 7–11 August 1989.

EEZ-Scan 85 Scientific Staff. 1987. *Atlas of the U.S. Exclusive Economic Zone, Gulf of Mexico and Eastern Caribbean Areas*. U.S. Geological Survey Miscellaneous Investigations I-1864-A.

Gauger S., Kuhn G., Gohl K., Feigl T., Lemenkova P., Hillenbrand C. 2007. Swath-bathymetric mapping. *Reports on Polar and Marine Research* 557, 38–45.

GDAL/OGR contributors (2020). GDAL/OGR Geospatial Data Abstraction software Library. Open Source Geospatial Foundation. Online: https://www.gdal.org (access: 4.07.2020).

GEBCO Compilation Group 2020. GEBCO 2020 Grid. https://doi.org/10.5285/a29c5465-b138-234d-e053-6c86abc040b9

Gómez G. 1996. Causa de la fertilidad marina en el nororiente de Venezuela. *Interciencia* 21(3), 140–146.

Granja Bruña J.L., ten Brink U.S., Carbó-Gorosabel A., Muñoz-Martín A., Gómez Ballesteros M. 2009. Morphotectonics of the Central Muertos thrust belt and Muertos Trough (Northeastern Caribbean). *Marine Geology* 263(1), 7–33. https://doi.org/10.1016/j.margeo.2009.03.010

Harris P.T., Macmillan-Lawler M. 2017. Origin and geomorphic characteristics of ocean basins. In: A. Micallef, S. Krastel, A. Savini (eds.), *Submarine Geomorphology*. *Geology*. Cham: Springer. https://doi.org/10.1007/978-3-319-57852-1_8

Hayes J.A., Larue D.K., Joyce J., Schellekens J.H. 1986. Puerto Rico: Reconnaissance study of the maturation and source rock potential of an oceanic arc involved in a collision. *Marine and Petroleum Geology* 3(2), 126–138. https://doi.org/10.1016/0264-8172(86)90024-3

Heezen B.C., Tharp M. 1961. *Physiographic Diagram of the South Atlantic, the Caribbean, the Scotia Sea, and the Eastern Margin of the South Pacific Ocean*. Geological Society of America.

Holcombe T.L., Ladd J.W., Westbrook G., Edgar N.T., Bowland C.L. 1990. Caribbean marine geology: Ridges and basins of the plate interior. In: G. Dengo, J.E. Case (eds.), *The Geology of North America.* Vol. H: *The Caribbean Region* (pp. 231–260). Boulder: Geological Society of America. https://doi.org/10.1130/DNAG-GNA-H

Jamieson A.J., Stewart H.A., Nargeolet P.-H. 2020. Exploration of the Puerto Rico Trench in the mid-twentieth century: Today's significance and relevance. *Endeavour* 44(1–2). https://doi.org/10.1016/j.endeavour.2020.100719

Jolly W.T, Lidiak E.G., Dickin A.P. 2008. Bimodal volcanism in northeast Puerto Rico and the Virgin Islands (Greater Antilles Island Arc): Genetic links with Cretaceous subduction of the mid-Atlantic ridge Caribbean spur. *Lithos* 103(3–4), 393–414. https://doi.org/10.1016/j.lithos.2007.10.008

Keppie J.D., Morán-Zenteno D.J. 2012. An alternative Pangea reconstruction for Middle America with the Chortis Block in the Gulf of Mexico: Tectonic implications. *International Geology Review* 54(14), 1685–1696. https://doi.org/10.1080/00206814.2012.676361

Klaucke I., Masson D.G., Petersen C.J., Weinrebe W., Ranero C.R. 2008. Multifrequency geoacoustic imaging of fluid escape structures offshore Costa Rica: Implications for the quantification of seep processes. *Geochemistry, Geophysics, Geosystems* 9(4). https://doi.org/10.1029/2007gc001708

Klaučo M., Gregorová B., Stankov U., Marković V., Lemenkova P. 2013a. Determination of ecological significance based on geostatistical assessment: A case study from the Slovak Natura 2000 protected area. *Central European Journal of Geosciences* 5(1), 28–42. https://doi.org/10.2478/s13533-012-0120-0

Klaučo M., Gregorová B., Stankov U., Marković V., Lemenkova P. 2013b. Interpretation of landscape values, typology and quality using methods of spatial metrics for ecological planning. *54th International Conference Environmental & Climate Technologies*. Riga, Latvia. https://doi.org/10.13140/RG.2.2.23026.96963

Klaučo M., Gregorová B., Stankov U., Marković V., Lemenkova P. 2014. Landscape metrics as indicator for ecological significance: Assessment of Sitno Natura 2000 sites, Slovakia. *Ecology and Environmental Protection. Proceedings of the International Conference* (pp. 85–90). March 19–20, 2014. Minsk, Belarus. https://doi.org/10.6084/m9.figshare.7434200

Klaučo M., Gregorová B., Stankov U., Marković V., Lemenkova P. 2017. Land planning as a support for sustainable development based on tourism: A case study of Slovak Rural Region. *Environmental Engineering and Management Journal* 2(16), 449–458. https://doi.org/10.30638/eemj.2017.045

Kuhn G., Hass C., Kober M., Petitat M., Feigl T., Hillenbrand C.D., Kruger S., Forwick M., Gauger S., Lemenkova P. 2006. The response of quaternary climatic cycles in the South-East Pacific: development of the opal belt and dynamics behavior of the West Antarctic ice sheet. In: K. Gohl (ed.), *Expedition programme No. 75 ANT XXIII/4, AWI Helmholtz Centre for Polar and Marine Research*. https://doi.org/10.13140/RG.2.2.11468.87687

Ladd J.W., Holcombe T.L., Westbrooke G.K., Edgar N.T. 1990. *Caribbean marine geology: Active margins of the plate boundary*. In: G. Dengo, J.E. Case (eds.), *The Geology of North America*. Vol. H: *The Caribbean Region* (pp. 261–290). Boulder: Geological Society of America.

Langlois A., Phipps M. 1997. *Automates cellulaires. Application à la simulation urbaine*. Paris: Hermès.

Lemenkova P. 2011. *Seagrass Mapping and Monitoring Along the Coasts of Crete, Greece*. M.Sc. Thesis. Netherlands: University of Twente. https://doi.org/10.13140/RG.2.2.16945.22881

Lemenkova P., Promper C., Glade T. 2012. Economic assessment of landslide risk for the Waidhofen a.d. Ybbs Region, Alpine Foreland, Lower Austria. In: E. Eberhardt, C. Froese, A.K. Turner, S. Leroueil (eds.), *Protecting Society through Improved Understanding. 11th International Symposium on Landslides & the 2nd North American Symposium on Landslides & Engineered Slopes (NASL)* (pp. 279–285). June 2–8, 2012. Banff, Canada. https://doi.org/10.6084/m9.figshare.7434230

Lemenkova P. 2018. R scripting libraries for comparative analysis of the correlation methods to identify factors affecting Mariana Trench formation. *Journal of Marine Technology and Environment* 2, 35–42. https://doi.org/10.6084/m9.figshare.7434167

Lemenkova P. 2019a. Geomorphological modelling and mapping of the Peru-Chile Trench by GMT. *Polish Cartographical Review* 51(4), 181–194. https://doi.org/10.2478/pcr-2019-0015

Lemenkova P. 2019b. Topographic surface modelling using raster grid datasets by GMT: Example of the Kuril-Kamchatka Trench, Pacific Ocean. *Reports on Geodesy and Geoinformatics* 108, 9–22. https://doi.org/10.2478/rgg-2019-0008

Lemenkova P. 2019c. GMT based comparative analysis and geomorphological mapping of the Kermadec and Tonga Trenches, Southwest Pacific Ocean. *Geographia Technica* 14(2), 39–48. https://doi.org/10.21163/GT_2019.142.04

Lemenkova P. 2019d. Automatic data processing for visualising Yap and Palau Trenches by generic mapping tools. *Cartographic Letters* 27(2), 72–89. https://doi.org/10.6084/m9.figshare.11544048

Lemenkova P. 2019e. Statistical analysis of the Mariana Trench geomorphology using R programming language. *Geodesy and Cartography* 45(2), 57–84. https://doi.org/10.3846/gac.2019.3785

Lemenkova P. 2019f. AWK and GNU octave programming languages integrated with generic mapping tools for geomorphological analysis. *GeoScience Engineering* 65(4), 1–22. https://doi.org/10.35180/gse-2019-0020

Lemenkova P. 2019g. Geophysical Modelling of the Middle America Trench using GMT. *Annals of Valahia University of Targoviste. Geographical Series* 19(2), 73–94. https://doi.org/10.6084/m9.figshare.12005148

Lemenkova P. 2020a. Variations in the bathymetry and bottom morphology of the Izu-Bonin Trench modelled by GMT. *Bulletin of Geography. Physical Geography Series* 18(1), 41–60. https://doi.org/10.2478/bgeo-2020-0004

Lemenkova P. 2020b. GMT based comparative geomorphological analysis of the Vityaz and Vanuatu Trenches, Fiji Basin. *Geodetski List* 74(97), 19–39. https://doi.org/10.6084/m9.figshare.12249773

Lemoine F.G., Kenyon S.C., Factor J.K., Trimmer R.G., Pavlis N.K., Chinn D.S., Cox C.M., Klosko S.M., Luthcke S.B., Torrence M.H., Wang Y.M., Williamson R.G., Pavlis E.C., Rapp R.H., Olson T.R. 1998. *The Development of the Joint NASA GSFC and NIMA Geopotential Model*

EGM96. NASA Goddard Space Flight Center, Greenbelt, Maryland, 20771 USA. Online: https://cddis.nasa.gov/926/egm96/nasatm.html (access: 11.11.2020).

Lindh P. 2004. *Compaction and strength properties of stabilised and unstabilised fine-grained tills*. PhD Thesis. Lund: Lund University. https://doi.org/10.13140/RG.2.1.1313.6481

Meschede M., Frisch W. 2002. The evolution of the Caribbean Plate and its relation to global plate motion vectors: Geometric constraints for an Inter-American origin. In: T.A. Jackson (ed.), *Caribbean Geology into the Third Millennium. Transactions of the 15th Caribbean Geological Conference* (pp. 1–14). Kingston: University of West Indies Press.

Micallef A., Krastel S., Savini A. 2018. *Submarine Geomorphology*. Springer Geology. Switzerland: Springer International Publishing AG. https://doi.org/10.1007/978-3-319-57852-1

Patriat M., Pichot T., Westbrook G.K., Umber M., Deville E., Benard F., Roest W.R., Loubrieu B. 2011. Evidence for quaternary convergence across the North America-South America plate boundary zone, east of the Lesser Antilles. *Geology* 39(10), 979–982. https://doi.org/10.1130/G32474.1

Pavlis N.K., Holmes S.A., Kenyon S.C., Factor J.K. 2012. The development and evaluation of the Earth Gravitational Model 2008 (EGM2008). *Journal of Geophysical Research* 117, B04406. https://doi.org/10.1029/2011JB008916

Perfit M.R., Heezen B.C. 1978. The geology and evolution of the Cayman Trench. *Geological Society of America Bulletin* 89, 1155–1174. https://doi.org/10.1130/0016-7606(1978)89<1155:TGAEOT>2.0.CO;2

Perfit M.R., Heezen B.C., Rawson M., Donnelly T.W. 1980. Chemistry, origin and tectonic significance of metamorphic rocks from the Puerto Rico Trench. *Marine Geology* 34(3–4), 125–156. https://doi.org/10.1016/0025-3227(80)90069-9

Pindell J.L., Barrett S.F. 1990. Geological evolution of the Caribbean region: A plate-tectonic perspective. In: G. Dengo, J.E. Case (eds.), *The Geology of North America*. Vol. H: *The Caribbean Region* (pp. 405–432). Geological Society of America. https://doi.org/10.1130/DNAG-GNA-H.405

Pinet P.R. 1976. Morphology off northern Honduras, northwestern Caribbean Sea. *Deep Sea Research and Oceanographic Abstracts* 23(9), 839–847. https://doi.org/10.1016/0011-7471(76)90851-2

Protti M., Gündel F., McNally K. 1994. The geometry of the Wadati-Benioff zone under southern Central America and its tectonic significance: Results from a high-resolution local seismographic network. *Physics of the Earth and Planetary Interiors* 84(1–4), 271–287. https://doi.org/10.1016/0031-9201(94)90046-9

Roobol M.J., Wright J.V., Smith A.L. 1983. Calderas or gravity-slide structures in the Lesser Antilles island arc? *Journal of Volcanology and Geothermal Research* 19(1–2), 121–134. https://doi.org/10.1016/0377-0273(83)90128-2

Rosencrantz E., Sclater J.G. 1986. Depth and age in the Cayman Trough. *Earth and Planetary Science Letters* 79, 133–144. https://doi.org/10.1016/0012-821X(86)90046-4

Rosencrantz E., Ross M.I., Sclater J.G. 1988. The age and spreading history of the Cayman Trough as determined from depth, heat flow, and magnetic anomalies. *Journal of Geophysical Research* 93, 2141–2157. https://doi.org/10.1029/JB093iB03p02141

__1

Rosencrantz M., Mann P. 1991. SeaMARC II mapping of transform faults in the Cayman Trough, Caribbean Sea. *Geology* 19(7), 690–691. https://doi.org/10.1130/0091-7613(1991)019<0690:SIMOTF>2.3.CO;2

Rousseeuw P.J. 1984. Least Median of Squares Regression. *Journal of the American Statistical Association* 79(388), 871–880. https://doi.org/10.1080/01621459.1984.10477105

Sanders L. 1989. *L'analyse statistique des données en géographie*. Montpellier: Alidade Reclus.

Sandwell D.T., Smith W.H.F. 1997. Marine gravity anomaly from Geosat and ERS 1 satellite altimetry. *Journal of Geophysical Research* 102, 10039–10054. https://doi.org/10.1029/96JB03223

Sandwell D.T., Müller R.D., Smith W.H.F., Garcia E., Francis R. 2014. New global marine gravity model from CryoSat-2 and Jason-1 reveals buried tectonic structure. *Science* 346(6205), 65–67. https://doi.org/10.1126/science.1258213

Schell B.A., Tarr A.C. 1978. Plate tectonics of the northeastern Caribbean. *Geologie en Mijnbouw* 57, 319–24.

Schenke H.W., Lemenkova P. 2008. Zur Frage der Meeresboden-Kartographie: Die Nutzung von AutoTrace Digitizer für die Vektorisierung der Bathymetrischen Daten in der Petschora-See. *Hydrographische Nachrichten* 81, 16–21. https://doi.org/10.6084/m9.figshare.7435538

Schmidt W.E., Siegel E. 2011. Free descent and on bottom ADCM measurements in the Puerto Rico Trench, 19.77°N, 67.40°W. *Deep Sea Research Part I: Oceanographic Research Papers* 58(9), 970–977. https://doi.org/10.1016/j.dsr.2011.06.005

Sclater J.G., Hellinger S., Tapscott C. 1977. The paleobathymetry of the Atlantic Ocean from the Jurassic to the Present. *The Journal of Geology* 85(5), 509–552.

Shepard F.P. 1963. *Submarine Geology*. New York: Harper & Row 557 p.

Shibata T. 1979. Pigeonite-bearing basalts dredged from the Puerto Rico Trench: A microprobe study. *Marine Geology* 30(3–4), 285–297. https://doi.org/10.1016/0025-3227(79)90020-3

Smith W.H.F., Sandwell D.T. 1997. Global seafloor topography from satellite altimetry and ship depth soundings. *Science* 277, 1956–1962. https://doi.org/10.1126/science.277.5334.1956

Straume E.O., Gaina C., Medvedev S., Hochmuth K., Gohl K., Whittaker J.M., Abdul Fattah R., Doornenbal J.C., Hopper J.R. 2019. GlobSed: Updated total sediment thickness in the world's oceans. *Geochemistry, Geophysics, Geosystems* 20(4), 1756–1772. https://doi.org/10.1029/2018GC008115

Suetova I.A., Ushakova L.A., Lemenkova P. 2005. Geoinformation mapping of the Barents and Pechora Seas. *Geography and Natural Resources* 4, 138–142. https://doi.org/10.6084/m9.figshare.7435535

ten Brink U. 2005. Vertical motions of the Puerto Rico Trench and Puerto Rico and their cause. *Journal of Geophysical Research* 110, 1–16. https://doi.org/10.1029/2004JB003459

Thomas I. 2001. Cartographie d'aujourd'hui et de demain: rappels et perspectives. *Cybergeo* 189, 17. https://doi.org/10.4000/cybergeo.3812

Tobler W.R. 1975. Mathematical map models. *International Symposium on Computer-Assisted Cartography*, Reston.

Tobler W.R. 1980. Statistical cartography: What is it? *Proceedings, Auto-Carto* IV, I. Reston.

Tsoulos L., Stefanakis C. 2005. *Development of a Cartographic Expert System*.

Wessel P., Smith W.H.F. 1991. Free software helps map and display data. *Eos Transactions AGU* 72(41), 441. https://doi.org/10.1029/90EO00319

Wessel P., Smith W.H F., Scharroo R., Luis J.F., Wobbe F. 2013. Generic mapping tools: Improved version released. *Eos Transactions AGU* 94(45), 409–410.

Wessel P., Smith W.H.F. 2018. *The Generic Mapping Tools. Version 4.5.18 Technical Reference and Cookbook*. Computer software manual. USA.

Wessel P., Luis J.F., Uieda L., Scharroo R., Wobbe F., Smith W.H.F., Tian D. 2019. The generic mapping tools version 6. *Geochemistry, Geophysics, Geosystems* 20, 5556–5564. https://doi.org/10.1029/2019GC008515

Wille P.C. 2005. *Sound Images of the Ocean in Research and Monitoring*. Heidelberg: Springer. https://doi.org/10.1007/3-540-27910-5

Wright J., Rothery D.A. 1998. *The Ocean Basins: Their Structure and Evolution*. 2nd ed. Milton Keynes: Elsevier.